Bioorganic & Medicinal Chemistry 18 (2010) 190–201

Contents lists available at ScienceDirect

Bioorganic & Medicinal Chemistry

journal homepage: www.elsevier.com/locate/bmc

Modulation of Wnt signaling through inhibition of secreted frizzled-related protein I (sFRP-1) with N-substituted piperidinyl diphenylsulfonyl sulfonamides: Part II

William J. Moore [a,*], Jeffrey C. Kern [a], Ramesh Bhat [b], Peter V. N. Bodine [b], Shoichi Fukyama [b], Girija Krishnamurthy [a], Ronald L. Magolda [a], Keith Pitts [a], Barb Stauffer [b], Eugene J. Trybulski [a]

[a] Chemical Sciences, Wyeth Research, 500 Arcola Road, Collegeville, PA 19426, United States
[b] Women's Health and Musculoskeletal Biology, Wyeth Research, 500 Arcola Road, Collegeville, PA 19426, United States

ARTICLE INFO

Article history:
Received 24 September 2009
Revised 29 October 2009
Accepted 2 November 2009
Available online 6 November 2009

Keywords:
Secreted-frizzled related protein-1 (sFRP-1)
Wnt pathway
Osteoblasts
Osteoporosis

ABSTRACT

Piperidinyl diphenylsulfonyl sulfonamides are a novel class of molecules that have inhibitory binding affinity for sFRP-1. As a secreted protein sFRP-1 inhibits the function of the secreted Wnt glycoprotein. Therefore, as inhibitors of sFRP-1 these small molecules facilitate the Wnt/β-catenin canonical signaling pathway. Details of the structure–activity relationships and biological activity of this structural class of compounds will be discussed.

1. Introduction

Secreted Wnt glycoproteins are responsible for activation of the Wnt signaling pathway. This signaling process is responsible for the regulation of various cellular developmental processes including cell proliferation, differentiation, and apoptosis which has been the topic of several recent reviews.[1–3] The Wnt/β-catenin canonical signaling pathway is initiated by the extracellular binding of Wnt to a membrane receptor complex composed of a Frizzled (Fzd) GPCR and a low-density lipoprotein receptor-related protein (LRP). The binding results in a signaling cascade leading to the stabilization of β-catenin, which translocates to the nucleus, resulting in the activation of transcriptional factors.[1,2,4] There are many regulators of the Wnt signaling process, including extracellular components such as WIF-1, Dkk-1, SOST, and secreted Frizzled-Related Protein-1 (sFRP-1 or SARP-2).[4,5] The sFRPs are one of the largest families of Wnt antagonists and share high homology to the membrane bound frizzled receptor. Human sFRP-1 is a 35 kD glycosylated protein consisting of 313 amino acids and eight disulfide linkages, five of which are located in the cysteine rich domain (CRD) while the remaining three disulfide bonds are located within the netrin domain.[6] sFRP-1, via the CRD domain, competes with the Fzd receptor for Wnt. Thus sFRP-1 is a negative regulator or an antagonist of the Wnt signaling pathway.[7a] Therefore, inhibitors

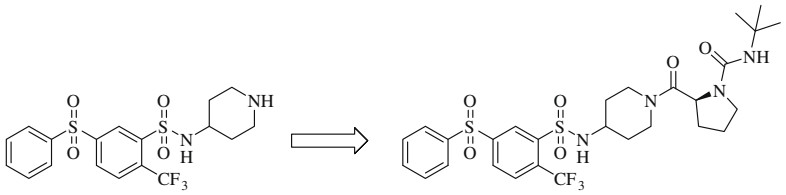

1 (WAY-316606)
FP Binding IC_{50} 0.5 μM
Wnt-luc EC_{50} 0.65 μM

2 (WAY-362692)
FP Binding IC_{50} 0.02 μM
Wnt-luc EC_{50} 0.03 μM

* Corresponding author. Tel.: +1 484 865 7827; fax: +1 484 865 9399.
E-mail address: moorew2@wyeth.com (W.J. Moore).

0968-0896/$ - see front matter © 2009 Elsevier Ltd. All rights reserved.
doi:10.1016/j.bmc.2009.11.002

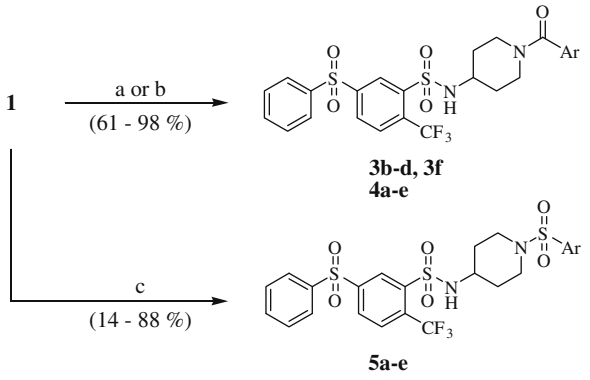

Scheme 1. See Table 1 for aryl (Ar) definitions. Reagents: (a) ArCOCl, TEA; (b) $ArCO_2H$, EDC, DMAP; (c) $ArSO_2Cl$, TEA.

of sFRP-1 could be pharmacologically useful agents for bone disorders like osteoporosis or fracture repair in which activation of the Wnt signaling pathway would be beneficial.[7b,c] Recently, the discovery of the diphenylsulfonyl sulfonamide scaffold was reported followed by a detailed account of the piperidinyl diphenylsulfonyl sulfonamide **1** (WAY-316606) and L-proline derived urea **2** (WAY-362692).[8,9] Compound **2** exhibited binding affinity (IC_{50} 20 nM) to the sFRP-1 protein and potent functional activity in both the cell-based functional assay (EC_{50} 30 nM) and the ex vivo mouse calvaria tissue culture.[9,11,12] During the course of the SAR investigations functionality was identified that could be substituted on the piperidinyl group to expand the SAR knowledge about the target as well as improve the chemical properties of the series. Herein, we highlight the synthesis and SAR of our efforts to expand the piperidinyl diphenylsulfonyl sulfonamide scaffold as sFRP-1 inhibitors.

2. Chemistry

The synthesis of compound **1** was described, including the detailed preparation of sulfonyl chloride **9**.[9] The synthetic routes illustrating the preparation of N-substituted piperidinyl diphenylsulfonyl sulfonamides **3–8** are shown in Schemes 1–3.

Treatment of **1** with an aryl or heteroaryl acid chloride, aryl sulfonyl chloride or activated aryl carboxylic acid in the presence of an amine base afforded amides **3b–d**, **3f 4a–e** and sulfonamides **5a–e**, respectively in moderate to good yields (Scheme 1). Alternatively, amide derivatives **3a**, **3e** or **4f–h** could be derived from the reaction of sulfonyl chloride **9** and the appropriately substituted 4-aminopiperidinyl carboxamides (Scheme 2). The aromatic nitrile **5d** was converted to the tetrazole **5e** following a convenient procedure described by Huff involving the reaction of an aryl nitrile with azidotrimethylsilane in the presence of the Lewis acid trimethylaluminum (Scheme 3).[13]

As shown in Scheme 4, compounds **6a** and **6b** were furnished albeit in modest yields via copper catalyzed N-arylation between **1** and the *meta*- or *para*-substituted boronic acids of tertiary butyl

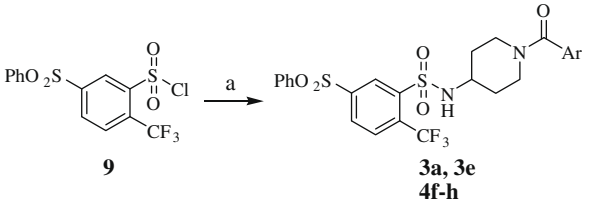

Scheme 2. Reagents and conditions: (a) (4-aminopiperidin-1-yl) arylcarbonyl, TEA, CH_2Cl_2 (23–76%).

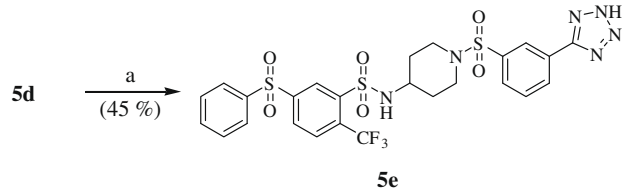

Scheme 3. Reagents and condition: (a) TMS–N_3, $Al(CH_3)_3$, toluene, 80 °C.

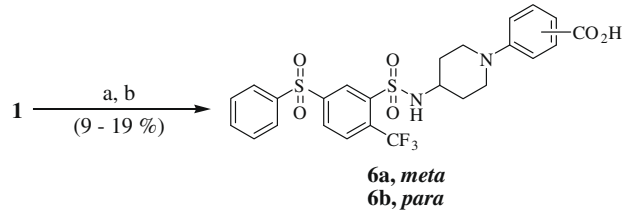

Scheme 4. Reagents and conditions: (a) 3- or 4-(*tert*butoxycarbonyl)phenylboronic acid, $Cu(OAc)_2$, TEA; (b) HCl, EtOAc or dioxane.

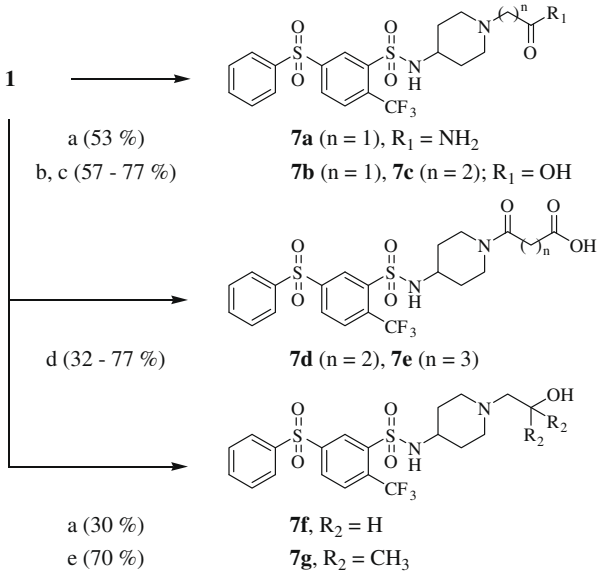

Scheme 5. Reagents and conditions: (a) 2-bromoethanol or 2-bromoacetamide, TEA; (b) *tert*-butyl 2-bromoacetate or *tert*-butyl 3-bromopropionate, TEA; (c) HCl, EtOAc or dioxane; (d) succinic or glutaric anhydride, EtOH, μ wave, 150 °C; (e) isobutylene oxide, EtOH, 75 °C.

benzoate. The tertiary butyl esters were further treated with acid to provide hydrochloride salts of the corresponding benzoic acid isomers.

The syntheses of derivatives **7a–g** are illustrated in Scheme 5. Alkylation of **1** at elevated temperatures with primary alkyl bromides in the presence of an acid scavenger such as triethylamine afforded compounds **7a** ($n = 1$, $R_1 = NH_2$) and **7f** ($R_2 = H$), respectively. Treatment of **1** in a similar manner, with the tertiary butyl esters of 2-bromoacetic acid or 3-bromopropionic acid followed by acidic hydrolysis provided the aliphatic carboxylic acids ($R_1 = OH$) **7b** ($n = 1$) and **7c** ($n = 2$). Alternatively, the tertiary alcohol **7g** ($R_2 = CH_3$) can be prepared by alkylating **1** with the epoxide of isobutylene. Reaction of **1** in an ethanolic solution containing either succinic or glutaric anhydride was facilitated by employing microwave irradiation affording the amido acids **7d** ($n = 2$) and **7e** ($n = 3$).

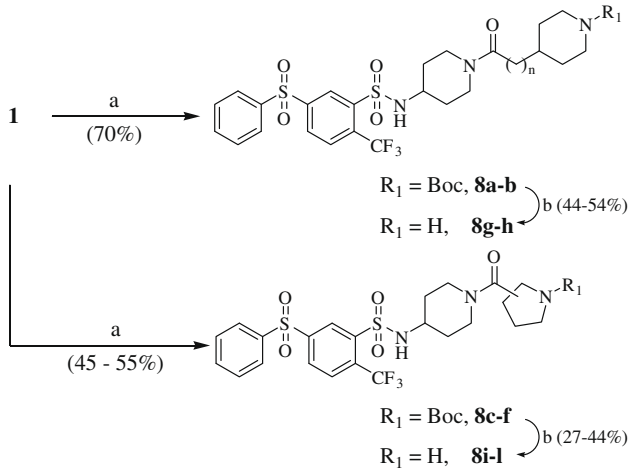

Scheme 6. Reagents: (a) CDI, TEA or EDC, DMAP; (b) HCl, EtOAc or dioxane.

The synthesis of *N*-Boc protected and deprotected *R*- and *S*-proline enantiomers **8c–d** and **8i–j** have been previously reported.[9] The remaining heterocycloalkyl derivatives were obtained in a similar manner starting with commercially available *N*-*tert*-butoxy carbonyl protected piperidine-4-carboxylic acid, piperidin-4-ylacetic acid, and the *R* or *S*-enantiomers of pyrrolidine-3-carboxylic acid. As depicted in Scheme 6, the acids were activated using standard procedures mediated by either carbonyl diimidazole (CDI) and triethylamine or *N*-(3-dimethylaminopropyl)-*N*′-ethylcarbodiimide (EDC) and *N*,*N*-dimethylaminopyridine (DMAP). When the activated acids were coupled with compound **1**, piperidinyl **8a–b** or pyrrolidinyl **8c–f** amides were provided. The deprotected analogs **8g–l** were acquired in good yields upon exposure to acid yielding the corresponding hydrochloride salts.

3. Results and discussion

Recent disclosures of the diphenylsulfonyl sulfonamide scaffold as sFRP-1 inhibitors have been reported.[8,9,11,12] Substitution on the piperidinyl group of the 4-sulfonamidopiperidinyl derivative **1** resulted in inhibitors, such as compound **2**, which possessed potent binding affinity to sFRP-1 as well as improved potency in our cell and tissue based assays.[9] These results prompted us to explore further optimization. Expansion of the N-substituted diphenylsulfone sulfonamide scaffold was facilitated by the use of **1** as an intermediate core from which several amides, sulfonamides, *N*-aryl and alkylated derivatives were prepared. A competitive binding assay as well as a cellular functional assay were devised to evaluate the small molecule inhibitors. The binding affinity of the compounds to purified sFRP-1 protein was initially determined using a tryptophan quenching assay. A rapid and more efficient competitive binding assay was developed using a fluorescein derivative of compound **1**.[10,11c] The cellular assay was derived from a U2-OS cell line that was virally infected with human sFRP-1, Wnt-3, and a TCF luciferase reporter. The cell-based activity (Wnt signaling) was measured as a function of luciferase production (fold induction, FI) after incubation of the cells with a test compound for 16–18 h. The functional activity was assessed in a dose–response format (EC_{50}). As a means of comparing the relative activity, constant fold induction thresholds were selected and the concentration of the sFRP-1 inhibitor was monitored. The fold induction constant values were extrapolated from the dose–response curve. Generally, there was good correlation between the binding affinity (IC_{50}) and the functional dose–response assays. In addition to the target profile, solubility, cytochrome *p*450 inhibition, and microsomal stability were also monitored to prioritize compounds with drug-like properties. Select compounds were further profiled in an ex vivo mouse calvaria tissue model of bone formation.

Tables 1–3 summarize the in vitro binding and functional activity profiles of the prepared sFRP-1 inhibitors. As the SAR around the piperidinyl diphenylsulfonyl sulfonamide developed, it became apparent that optimized substitutions to the growing scaffold resulted in molecules that began to resemble peptidomimetic-like structures. Due to the protein–protein relationship between sFRP-1 and Wnt, it was not unreasonable to expect that higher molecular weight compounds would be required to perturb the interaction and influence the functional activity.

An unsubstituted aryl group adjoined to the piperidine by either carbonyl **3a** (IC_{50} 0.07 μM, EC_{50} 0.25 μM) or sulfonyl **5a** (IC_{50} 0.13 μM, EC_{50} 0.21 μM) were equivalent in binding affinity and potency (Tables 1 and 3). Chloro substitution on the phenyl at the *ortho* (**3b**), *meta* (**3c**), or *para* (**3d**) positions resulted in derivatives exhibiting a 2.5–5-fold loss in activity relative to the unsubstituted derivative **3a**. Additional *para*-substituted compounds bearing the trifluoromethyl **3e** and dimethylamino **3f** were similarly characterized as sFRP-1 inhibitors with moderate binding affinities (>0.2 μM) and functional activity (0.2–1.9 μM) and offered no advantages over the parent molecule **3a**. Positioning of a nitrogen atom within the aromatic ring relative to the carbonyl was most effective at the 2- or 3-positions, while substitution at the 4-position provide an sFRP-1 inhibitor with weaker binding and functional activity. The pyridyl derivatives **4b** (IC_{50} 0.06 μM, EC_{50} 0.23 μM) and **4c** (IC_{50} 0.08 μM, EC_{50} 0.12 μM) had comparable binding affinity and functional activity while the *para*-situated compound **4a** (IC_{50} 0.20 μM, EC_{50} 0.60 μM) had 2.5–4.5-fold less activity in either binding or functional response. Further substitution of **4c** led to compounds containing chloro (**4d**), trifluoromethyl (**4e**) and dimethylamino (**4f**) groups and resulted in compounds with similar binding affinity and functional activity. It should be noted that while compound **4f** (IC_{50} 0.04 μM, EC_{50} 0.07 μM) demonstrated analogous binding affinity to the initial phenyl derivative **3a** (IC_{50} 0.07 μM, EC_{50} 0.25 μM) it exhibited a fourfold improvement in functional potency. The fold induction response (2- and 4-FI) in the functional assay provided alternate functional evidence of these derivatives ability to modulate Wnt signaling. Four of the 3-pyridyl analogs (**4c–f**) invoked a fourfold induction of luciferase signal at concentrations of 0.2 μM or less. Additional amino pyridinyl derivatives of **4f** that reduced the number of rotatable bonds while increasing the steric bulk were explored. A decline in binding and functional activity was observed with 3-pyridyl derivatives in which the dimethylamino group of **4f** was replaced with heterocycles such as the pyrrolidino **4g** (IC_{50} 0.87 μM, EC_{50} 0.23 μM) or morpholino **4h** (IC_{50} 0.13 μM, EC_{50} 0.14 μM).

Summarized in Table 2 for compounds **4c–h** are the calculated properties for the 'R' groups as well as the in vitro solubility and microsomal stability profiles of these compounds. The calculated molar refractivity (cMR) for compounds **4g** and **4h** increases significantly relative to analogs **4d–f**, which suggests that an increase in steric bulk may partially account for the decrease in binding affinity. However, a multivariate combination of molecular properties may account for the differentiation observed between **4g** and **4f**. In addition to an increase in the cMR, the *c* log *P* of the pyrrolidino group is increased whereas the morpholino group shares the same cMR value albeit with a *c* log *P* value analogous to compounds **4d–f**.

As demonstrated in Table 2, the pyridyl derivatives provided an ionizable group to facilitate aqueous solubility (**4c**, aqueous solubility 78 μM) while the substituted pyridyl targets exhibited diminished solubility in aqueous pH 7.4 buffer (<10 μM). As anticipated, the pyridyl derivatives possessed poor stability in phase I metabolizing microsomes, with the exception of the derivatives

Table 1
Comparison of aryl/heteroaryl carbonyl/sulfonyl derivatives **3a–f** and **4a–h** using fluorescence polarization binding and U2-OS functional activity assays

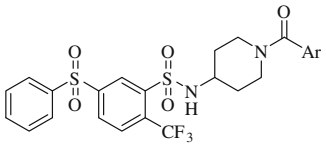

3a-f, 4a-h

Compound	Ar = phenyl	FP binding[a] (μM)		Wnt-luc[b] (μM)		
		IC_{50}	Max concn	EC_{50}	2-FI[c]	4-FI[c]
3a	H	0.07	12.5	0.25	0.24	NA[d]
3b	2-Cl	0.20	6.3	1.9	0.49	2.6
3c	3-Cl	0.30	6.3	0.87	0.49	1.4
3d	4-Cl	0.30	3.1	1.8	0.85	2.4
3e	4-CF_3	0.40	6.3	0.97	0.53	146
3f	4-$N(CH_3)_2$	0.30	50	0.19	0.15	NA[d]
	Ar = pyridine					
4a	4-yl	0.20	50	0.60	0.14	0.57
4b	2-yl	0.06	100	0.23	0.07	0.41
4c	3-yl	0.08	50	0.12	0.04	0.22
4d	6-Cl-3-yl	0.11	25	0.14	0.06	0.17
4e	6-(CF_3)-3-yl	0.05	12.5	0.14	0.02	0.16
4f	6-$N(CH_3)_2$-3-yl	0.04	12.5	0.07	0.03	0.18
4g	6-(Pyrrolidino)-3-yl	0.87	12.5	0.23	0.10	0.68
4h	6-(Morpholino)-3-yl	0.13	25	0.14	0.08	0.39

[a] The affinity of test compounds for sFRP-1 was determined using the FP binding assay. The dose–responses were run in duplicate and IC_{50}'s averaged. The mean confidence value (CV) for the binding assay IC_{50} determinations was ±15%.
[b] The osteosarcoma cell line, U2-OS, was used for the functional assay.
[c] Micromolar concentration that elicited a twofold (2-FI) or fourfold (4-FI) increase in Wnt signaling. Each point from the dose–response was measured in quadruplicate. The standard deviations for the Wnt-luc assay were typically ±9% of the mean or less.
[d] A fourfold induction of the luciferase signal was not achieved (NA).

Table 2
Calculated R-group properties, aqueous solubility and liver microsomal stability for 3-pyridinyl derivatives

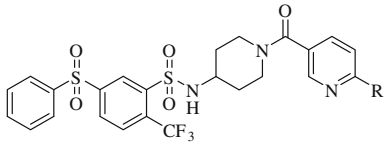

4c-h

Compound	R	R group properties[a]			Solubility pH 7.4[b] (μM)	Liver microsome $t_{1/2}$[c] (min)	
		c log *P*	cMR	PSA		Human	Rat
4c	H	0	0	0	78	6	2
4d	Cl	0.7	0.5	0	1.7	>30	9
4e	CF_3	0.9	0.5	0	3.2	>30	16
4f	$N(CH_3)_2$	0.7	1.3	3	6.7	3	2
4g	Pyrrolidin-1-yl	1.5	2.0	3	9.6	4	2
4h	Morpholin-4-yl	0.4	2.2	12	4.7	5	8

[a] Daylight method was used to calculate *c* log *P* and cMR values and PSAs were calculated from an internally developed algorithm.
[b] Solubility was assessed in an aqueous buffer from a DMSO stock solution.
[c] Human and rat liver microsomes were incubated with 1 μM DMSO stock solution of compounds.

containing electron withdrawing groups ($t_{1/2}$ >30 min). The trends emerging from the SAR were directing toward targets with suboptimal physical properties (e.g., limited aqueous solubility) thus we were prompted to examine an alternate ionizable groups to promote aqueous solubility. Functionality such as saturated heterocycles (**8**), alcohols (**7**) or deprotonatable species such as carboxylic acids (**5** or **6**) were investigated.

The saturated heterocyclic analogs shown in Table 3 (**8a–l**) are related to compound **2**. Compounds **8c** and **8i** were previously disclosed, are direct precursors to **2**, and were included for SAR comparison. In the case of the six-membered heterocycles, removal of the carbamate group resulted in 2.5–5-fold improved binding and functionally potent inhibitors, **8g** (IC_{50} 0.12 μM, EC_{50} 0.15 μM) and **8h** (IC_{50} 0.10 μM, EC_{50} 0.21 μM). The linker, n = 0 or 1, did not have a significant effect on target activity. The basic piperidinyl moiety in compounds **8g** and **8h** was fortuitous since this functionality provided improved aqueous solubility (>100 μM) as well as stability in the microsomal assay for rat and human (>30 min), as indicated in Table 4. Conversely, the pyrrolidine scaffold containing the tertiary butyl carbamate appendage was better suited relative to the basic secondary nitrogen. In the previous disclosure, we indicated that the *S*-enantiomer **8c** was favored, 2–3-fold, over

Table 3
Comparison of piperidinyl/pyrrolidinyl carbonyl derivatives **8a–l** using fluorescence polarization binding and U2-OS functional activity assays

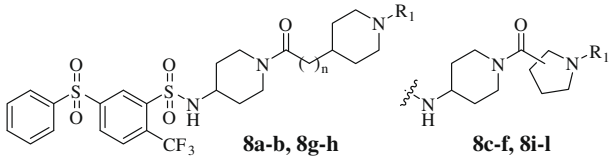

8a-b, 8g-h **8c-f, 8i-l**

Compound	*n*	R_1	Isomer	FP binding[a] (μM)		Wnt-luc[b] (μM)		
				IC_{50}	Max concn	EC_{50}	2-FI[c]	4-FI[c]
8a	0	Boc		0.30	25	0.42	0.28	NA
8b	1	Boc		0.49	12.5	0.40	0.16	0.52
8c		Boc	2*S*	0.06	25	0.06	0.02	0.16
8d		Boc	2*R*	0.12	25	0.21	0.09	0.97
8e		Boc	3*S*	0.07	25	0.15	0.06	0.26
8f		Boc	3*R*	0.05	12.5	0.08	0.03	0.14
8g	0	H		0.12	100	0.15	0.16	NA
8h	1	H		0.10	100	0.21	0.06	0.25
8i		H	2*S*	0.11	50	0.35	0.17	2.0
8j		H	2*R*	0.20	25	0.71	0.34	3.0
8k		H	3*S*	0.04	25	0.70	0.22	2.1
8l		H	3*R*	0.06	12.5	0.38	0.12	1.6

[a–c] See Table 1.

Table 4
Aqueous solubility and microsomal stability for heterocyclic derivatives

Compound	Solubility pH 7.4[a] (μM)	Liver microsome $t_{1/2}$[b] (min)	
		Human	Rat
8g	>100	>30	>30
8h	>100	>30	>30
8i	>100	19	24
8j	>100	15	9
8k	77	>30	>30
8l	70	NA	>30

[a,b] See Table 2.

the *R*-enantiomer but not to the extent that was traditionally observed in a eutomer/distomer relationship of a targeted receptor. We also described substitutions that were tolerated on this group that resulted in the identification of **2**. The binding and functional data for stereo isomers **8e** and **8f**, indicated that a modest chiral bias, albeit in favor of the *R*-isomer. The assignment of stereochemistry based on commercially available chiral intermediates and the procedures used to couple the two entities would not be expected to invert the established stereochemistry. Also consistent with our earlier disclosure, the carbamates or acylated derivatives had limited aqueous solubility. The carbamate also rendered these derivatives with lower stability in liver microsomes. Alternatively, the deprotected derivatives **8g–l** generally demonstrated moderate to good aqueous solubility (77 to >100 μM) and like the piperidinyl analogs were stable in the presence of liver microsomes. Interestingly, the regioisomers from the 3-substituted pyrrolidine moiety (**8k**, **8l**) were more stable ($t_{1/2}$ >30 min) in the microsomal stability assay than the 2-substituted isomers (**8i**, **8j**).

Substituted aryl sulfonamides and a direct linked *N*-aryl group containing a carboxyl group at either the *meta* (**5b**, **6a**) or *para* (**5c**, **6b**) positions were evaluated and the data is summarized in Table 5. The unsubstituted aryl sulfonamide **5a** exhibited relatively good binding and functional activity. Addition of a carboxylic acid at the *meta* **5b** or *para* **5c** positions was well tolerated and the two sulfonyl benzoic acid derivatives demonstrated equivalent binding affinity (IC_{50} 0.02 μM), 6.5-fold better than compound **5a** (IC_{50} 0.13 μM, EC_{50} 0.21 μM) while less than a two-fold separation differentiated the functional activity (EC_{50} 0.19 and 0.11 μM, respectively). Comparison of compounds **5b** or **5c**, to the direct linked or nonsulfonyl benzoic acids, **6a** and **6b**, demonstrated a 5–6-fold decrease in binding with only a slight decline in potency. The functional efficacy for acid derivatives **5b** and **6b** resulted in a fourfold induction at concentrations that were representative of the functional potency. Replacement of the carboxylic acid with the tetrazole moiety provided compound **5e**. The bioisostere had respectable binding affinity (IC_{50} 0.03 μM), but significantly decreased functional potency (EC_{50} 1.2 μM). The nitrile **5d** (IC_{50} 0.09 μM, EC_{50} 0.17 μM) possessed binding and functional activity that was comparable to the parent sulfonamide **5a** or the acids (**5b** and **5c**), the distinction was more pronounced in the concentration required to induce a fourfold induction (>0.5 μM).

The realization that a group such as a carboxylic acid was tolerated led to the design of targets intended to provide aqueous solubility while reducing the molecular weight. Table 6 summarizes the aliphatic *N*-alkyl derivatives as well as the *N*-acyl derivatives. The acids **7b**, **7d**, and **7e** exhibited moderate binding (IC_{50} 0.2–0.5 μM) to sFRP-1 and functional potency (EC_{50} 0.4–0.57 μM) that was more analogous to compound **1**. The drop in activity for com-

Table 5
Comparison of aryl/heteroaryl carbonyl/sulfonyl derivatives **3a–f** and **4a–i** using fluorescence polarization binding and U2-OS functional activity assays

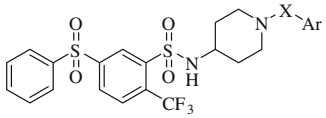

5a-e, 6a-b

Compound	X	Ar = phenyl	FP binding[a] (μM)		Wnt-luc[b] (μM)		
			IC_{50}	Max concn	EC_{50}	2-FI[c]	4-FI[c]
5a	SO_2	H	0.13	25	0.21	0.12	NA[e]
5b[d]	SO_2	3-CO_2H	0.02	12.5	0.19	0.083	0.18
5c	SO_2	4-CO_2H	0.02	12.5	0.11	0.10	NA[e]
5d	SO_2	3-CN	0.09	6.3	0.17	0.096	0.57
5e	SO_2	3-(Tetrazol-5-yl)	0.03	100	1.2	0.39	2.9
6a	Bond	3-CO_2H	0.10	100	0.35	0.27	0.41
6b	Bond	4-CO_2H	0.12	25	0.23	0.061	0.22

[a–c] See Table 1.
[d] Average from 13 independent dose response determinations.
[e] NA, data was not available.

Table 6
Comparison of alkyl/acylated carboxylic acids and alcohols **7a–g** using fluorescence polarization binding and U2-OS functional activity assays

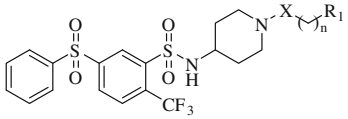

7a-g

Compound	*n*	R_1	X	FP binding[a] (μM)		Wnt-luc[b] (μM)		
				IC_{50}	Max concn	EC_{50}	2-FI[c]	4-FI[c]
7a	0	$CONH_2$	CH_2	0.06	100	0.31	0.18	NA
7b	0	CO_2H	CH_2	0.19	100	0.57	0.41	NA
7c	1	CO_2H	CH_2	0.9	100	1.2	0.99	NA[d]
7d	2	CO_2H	CO	0.27	25	0.40	0.35	NA
7e	3	CO_2H	CO	0.50	50	0.57	0.33	NA
7f	1	CH_2OH	CH_2	0.50	100	0.85	0.12	0.52
7g	1	$C(CH_3)_2OH$	CH_2	0.20	50	0.63	0.15	0.64

[a–c] See Table 1.
[d] Maximum fold induction achieved was 3-FI at 19 μM.

Table 7
Aqueous solubility and microsomal stability for carboxylic acids and alcohols

Compound	Solubility pH 7.4[a] (μM)	Liver microsome $t_{1/2}$[b] (min)	
		Human	Rat
5b	>100	>30	23
6a	>100	>30	17
7b	90	>30	>30
7d	95	>30	>30
7f	>100	3	7
7g	>100	<1	3

[a] Solubility was assessed in an aqueous buffer from a DMSO stock solution.
[b] Human and rat liver microsomes were incubated with 1 μM DMSO stock solution of compounds.

Table 8
Anabolic activity of sFRP-1 inhibitors demonstrated in an ex vivo calvaria tissue culture assay

Compound	Concentration (μM)	% Increase relative to control	
		TBA (SE)	OB #s (SE)
hPTH (1–34)	0.001	48 (19)[b]	87 (11)[a]
4c	0.1	65 (7)[a,d]	36 (8)[b]
4f	0.001	135 (21)[a,d]	78 (15)[b]
5b	0.001	56 (11)[a,d,f]	0
5c	0.001	49 (8)[a,e]	0
8h	0.001	47 (9)[b,e]	27 (5)[c]

[a] p <0.0001.
[b] p <0.01.
[c] p <0.05.
[d] Number of calvaria = 4.
[e] Number of calvaria = 5.
[f] Average of five experiments.

pound **7c** (IC_{50} 0.9 μM, EC_{50} 1.2 μM) relative to the corresponding derivatives was attributed to the proximity of the piperidinyl nitrogen to the acid. The two groups are situated to form a spirocyclic hydrogen bond, and a zwitterionic species that diminishes the interaction with the protein. Binding and functional activity were restored to levels comparable to **7b** when the acidity of the proton was reduced in the form of either a primary amide **7a** or as the primary or tertiary alcohols, **7f** and **7g**. The presence of a carboxylic acid group was desired to provide an opportunity to improve aqueous solubility and Table 7 highlights some selected acids and alcohols that were previously described. As expected, the aqueous solubility of the acid derivatives was generally good ($\geqslant$90 μM). The acids were associated with good stability in human and rat liver microsomes. The alcohols, **7f** and **7g**, provided improved aqueous solubility but little improvement in microsomal stability.

Select sFRP-1 inhibitors based on the potent activity observed in the functional assay, compounds **4c**, **4g**, **5b**, **5c**, and **8h** were evaluated in the ex vivo mouse calvaria assay.[14] As described in our previous disclosure, screening concentrations in the ex vivo assay were significantly lower than the observed in vitro potency. Evidence of anabolic activity such as increased bone formation and remodeling, osteoblast activation and differentiation, and increases in the osteoblast population were determined by histological assessment. Treatment of the calvaria with either 100 or 1 nM DMSO stock solutions of the sFRP-1 inhibitors resulted in significant increases in total bone area relative to the controls as shown in Table 8. For the three basic molecules **4c**, **4g**, and **8h** significant increases in osteoblast population were observed, whereas for the two aryl carboxylic acids, **5b** and **5c**, no increase in the osteoblast numbers was observed. In each treatment group the qualitative histology assessment indicated activation of the osteoblast cells and active bone remodeling. The significance of increasing osteoblast numbers in the ex vivo calvaria model and the relationship to bone related disease has not been rigorously established. However, typical treatment of the calvaria with hPTH(1–34) under the same conditions results not only in an increase in the total bone area, but also a dramatic increase in the number of osteoblast cells. Data from a representative experiment conducted with hPTH(1-34) are shown in Table 8 for comparison.

4. Conclusion

We have presented an expanded SAR disclosure of the piperidinyl diphenylsulfonyl sulfonamide scaffold. The in vitro and ex vivo data provided evidence of sFRP-1 inhibition, which modulated Wnt signaling through perturbation of the protein–protein interaction between Wnt and sFRP-1. Compound **1** (IC_{50} 0.5 μM, EC_{50} 0.65 μM) allowed us the opportunity to probe various functionality on the novel diphenylsulfonyl sulfonamide scaffold to improve the drug-like properties. Several compounds described herein have demonstrated potent binding affinity ($IC_{50} \leqslant 100$ nM) to the sFRP-1 protein. In a cell-based Wnt signaling assay many of the molecules demonstrated good binding affinity and potent functional activity (EC_{50} 70–150 nM). Five sFRP-1 inhibitors increased total bone area (47–135%) relative

to the vehicle control in an ex vivo mouse calvaria model, wherein parameters of anabolic activity such as activation of osteoblasts and active bone remodeling were observed. In particular, compound **4f** (IC_{50} 0.04 μM, EC_{50} 0.07 μM) demonstrated robust activity in the ex vivo model, not only increased total bone area (135%) but also promoted an increase in the population of bone forming osteoblasts (78%). Other aspects of anabolic activity such as osteoblast activation and active remodeling were also coupled with this activity. While compound **4f** had a good in vitro and ex vivo profile, it demonstrated low stability in the human and rat liver microsomal assays ($t_{1/2}$ 3 and 2 min, respectively) and would be predicted to have limited oral bioavailability due to first pass metabolism. Compound **8h** (IC_{50} 0.10 μM, EC_{50} 0.21 μM) demonstrated robust activity in the ex vivo model, also regulating bone formation (47%) as well as increasing OB numbers (27%). This piperidinyl derivative also demonstrated good aqueous solubility (>100 μM) and stability in the human and rat liver microsomal assays ($t_{1/2}$ >30 min). The benzoic acid derivative, **5b** (IC_{50} 0.02 μM, EC_{50} 0.19 μM) was also very active in the calvaria assay, but was ineffective at increasing the number of osteoblasts. Appending an acid group to the aryl sulfonamides also resulted in increased aqueous solubility (>100 μM) as well as improved microsomal stability affording extended half-lives in the rat (23 min) and human (>30 min) liver microsomal assays.[15] Future communications we will detail additional SAR studies of related scaffolds.

5. Experimental procedures

5.1. Chemistry

Solvents were purchased as anhydrous grade and used without further purification. Reagents were purchased from commercial sources and used as received. ^{1}H NMR spectra were recorded on a Varian Inova 400 instrument with chemical shifts reported in d values (parts per million, ppm) relative to an internal standard (tetramethylsilane). High-resolution mass spectra were obtained on an Agilent 6210 TOF. Low-resolution electrospray (ESI) mass spectra were recorded on an Aglient MSD. HPLC analyses were obtained on an Agilent 1200 using the following conditions: Waters Xterra RP18 HPLC column (3.5 μ, 150 mm L × 4.6 mm ID), 40 °C column temperature, 1.2 mL/min flow rate, photodiode array detection (210–370 nm), linear mobile phase gradient of 15–95% B over 10 min, holding 5 min at 95% B (mobile phase A: 10 mM ammonium formate in water, pH 3.5/mobile phase B: 1:1 methanol/acetonitrile).

5.1.1. General procedure for the coupling of an acid or sulfonyl chloride to 1 using triethylamine

To a stirred solution of **1** (0.22 mmol) in methylene chloride (3 mL) with triethylamine (0.70 mmol) was added ArCOCl or Ar-SO_2Cl (0.22 mmol) and the resulting solution was stirred overnight at room temperature. The reaction mixture was washed with water and concentrated. Product was purified using flash column separation using either a methylene chloride/methanol (1–10%) or hexane/ethyl acetate (5–50%) gradient.

5.1.2. General procedure for the carbonyldiimidazole coupling of an acid to 1 using triethylamine

The acid (0.70 mmol) was activated in the presence of CDI (0.68 mmol) and triethylamine (0.14 mmol) in DMF (2 mL) for 30 min followed by the addition of **1** (0.45 mmol). The resulting solution was heated to 100 °C for 15 min. The mixture was diluted with a saturated aqueous ammonium chloride solution and extracted several times with ethyl acetate. The combined organic layers were washed with brine several times, dried (Na_2SO_4), filtered and concentrated. Flash column separation using hexane/ethyl acetate (30–100% gradient provided the desired amide.

5.1.3. General procedure for the EDC coupling of an acid to 1 using triethylamine

To a stirred solution of 5-oxo-pyrrolidine-1,2-dicarboxylic acid 1-*tert*-butyl ester (0.075 g, 0.32 mmol) in methylene chloride (3 mL) was added DMAP (0.04 g, 0.32 mmol) and EDC (0.07 g, 0.035 mmol). The resulting solution was stirred at room temperature for 20 min at which time **1** (0.12 g, 0.27 mmol) was added and stirred overnight at room temperature. The reaction was washed with saturated aqueous ammonium chloride solution and concentrated. Flash column separation using 0–8% methanol/methylene chloride gradient gave **4c** (0.10 g, 56%).

5.1.3.1. *N*-(1-Benzoylpiperidin-4-yl)-5-(phenylsulfonyl)-2-trifluoromethyl)benzenesulfonamide (3a). ^{1}H NMR (400 MHz, DMSO-d_6) δ 8.61 (d, J = 6.50 Hz, 1H), 8.58 (d, J = 1.56 Hz, 1H), 8.41 (dd, J = 1.04, 8.32 Hz, 1H), 8.23 (d, J = 8.32 Hz, 1H), 8.00–8.05 (m, 2H), 7.59–7.72 (m, 3H), 7.43–7.50 (m, 3H), 7.32–7.38 (m, 2H), 4.20 (br s, 1H), 3.27–3.48 (m, 2H), 2.73–3.05 (m, 2H), 1.21–1.70 (m, 4H); MS (ES) m/z 553.1; HRMS: calculated for $C_{25}H_{23}F_3N_2O_5S_2 + H^+$, 553.10732; found (ESI, $[M+H]^+$), 553.1075; HPLC purity 98.6%, R_T 9.4 min.

5.1.3.2. *N*-[1-(2-Chlorobenzoyl)piperidin-4-yl]-5-(phenylsulfonyl)-2-(trifluoromethyl)benzenesulfonamide (3b). ^{1}H NMR (400 MHz, DMSO-d_6) δ 8.61 (dd, J = 7.54, 11.70 Hz, 1H), 8.57 (d, J = 1.56 Hz, 1H), 8.41 (dd, J = 1.17, 8.19 Hz, 1H), 8.23 (d, J = 8.58 Hz, 1H), 8.00–8.05 (m, 2H), 7.60–7.71 (m, 3H), 7.50–7.58 (m, 1H), 7.34–7.49 (m, 2H), 7.30 (dd, J = 1.82, 7.28 Hz, 1H), 4.18–4.32 (m, 1H), 3.29–3.42 (m, 1H), 3.02–3.15 (m, 1H), 2.76–2.98 (m, 2H), 1.57–1.66 (m, 1H), 1.19–1.49 (m, 3H); MS (ES) m/z 587.0; HRMS: calculated for $C_{25}H_{22}ClF_3N_2O_5S_2 + H^+$, 587.06835; found (ESI, $[M+H]^+$), 587.0666; HPLC purity 93.6%, R_T 9.6 min.

5.1.3.3. *N*-[1-(3-Chlorobenzoyl)piperidin-4-yl]-5-(phenylsulfonyl)-2-(trifluoromethyl)benzenesulfonamide (3c). ^{1}H NMR (400 MHz, DMSO-d_6) δ 8.56–8.64 (m, 2H), 8.38–8.45 (m, 1H), 8.23 (d, J = 8.32 Hz, 1H), 8.00–8.07 (m, 2H), 7.61–7.73 (m, 3H), 7.52–7.56 (m, 1H), 7.47–7.52 (m, 1H), 7.42 (t, J = 1.56 Hz, 1H), 7.31 (dt, J = 1.36, 7.41 Hz, 1H), 4.09–4.27 (m, 1H), 3.24–3.41 (m, 2H), 2.74–3.06 (m, 2H), 1.42–1.70 (m, 2H), 1.22–1.41 (m, 2H); MS (ES) m/z 587.0; HRMS: calculated for $C_{25}H_{22}ClF_3N_2O_5S_2 + H^+$, 587.06835; found (ESI, $[M+H]^+$), 587.0674; HPLC purity 98.4%, R_T 9.9 min.

5.1.3.4. *N*-[1-(4-Chlorobenzoyl)piperidin-4-yl]-5-(phenylsulfonyl)-2-(trifluoromethyl)benzenesulfonamide (3d). ^{1}H NMR (400 MHz, DMSO-d_6) δ 8.61 (d, J = 6.76 Hz, 1H), 8.58 (d, J = 1.82 Hz, 1H), 8.41 (dd, J = 1.04, 8.32 Hz, 1H), 8.23 (d, J = 8.32 Hz, 1H), 8.00–8.06 (m, 2H), 7.68–7.73 (m, 1H), 7.62–7.67 (m, 2H), 7.51–7.55 (m, 2H), 7.37–7.41 (m, 2H), 4.17 (br s, 1H), 3.26–3.49 (m, 2H), 2.72–3.08 (m, 2H), 1.43–1.70 (m, 2H), 1.22–1.41 (m, 2H); MS (ES) m/z 587.0; HRMS: calculated for $C_{25}H_{22}ClF_3N_2O_5S_2 + H^+$, 587.06835; found (ESI, $[M+H]^+$), 587.0698; HPLC purity 98.2%, R_T 9.9 min.

5.1.3.5. 5-(Phenylsulfonyl)-2-(trifluoromethyl)-*N*-{1-[4-(trifluoromethyl)benzoyl]piperidin-4-yl}benzenesulfonamide (3e). ^{1}H NMR (400 MHz, DMSO-d_6) δ 8.62 (br s, 1H), 8.58 (d, J = 1.82 Hz, 1H), 8.41 (dd, J = 1.17, 8.45 Hz, 1H), 8.23 (d, J = 8.32 Hz, 1H), 7.99–8.07 (m, 2H), 7.84 (d, J = 8.06 Hz, 2H), 7.61–7.73 (m, 3H), 7.58 (d, J = 7.80 Hz, 2H), 4.11–4.29 (m, 1H), 3.25–3.42 (m, 2H), 2.76–3.07 (m, 2H),

1.44–1.70 (m, 2H), 1.22–1.43 (m, 2H); MS (ES) *m/z* 621.1; HRMS: calculated for $C_{26}H_{22}F_6N_2O_5S_2 + H^+$, 621.09471; found (ESI, $[M+H]^+$), 621.0933; HPLC purity 100%, R_T 10.0 min.

5.1.3.6. *N*-{1-[4-(Dimethylamino)benzoyl]piperidin-4-yl}-5-(phenylsulfonyl)-2-(trifluoromethyl)benzenesulfonamide (3f). ^{1}H NMR (400 MHz, DMSO-d_6) δ 8.55–8.64 (m, 2H), 8.37–8.45 (m, 1H), 8.23 (d, *J* = 8.46 Hz, 1H), 7.99–8.07 (m, 2H), 7.60–7.73 (m, 3H), 7.20–7.28 (m, 2H), 6.76 (d, *J* = 8.46 Hz, 2H), 3.73–4.04 (m, 2H), 3.26–3.39 (m, 1H), 2.96 (s, 6H), 2.80–2.92 (m, 2H), 1.45–1.57 (m, 2H), 1.20–1.36 (m, 2H); MS (ES) *m/z* 595.8; HRMS: calculated for $C_{27}H_{28}F_3N_3O_5S_2 + H^+$, 596.14952; found (ESI, $[M+H]^+$), 596.1509; HPLC purity 95.8%, R_T 9.7 min.

5.1.3.7. 5-(Phenylsulfonyl)-*N*-[1-(pyridin-2-ylcarbonyl)piperidin-4-yl]-2-(trifluoromethyl)benzenesulfonamide (4a). ^{1}H NMR (400 MHz, DMSO-d_6) δ 8.64 (d, *J* = 7.43 Hz, 1H), 8.61 (ddd, *J* = 1.02, 1.79, 4.87 Hz, 1H), 8.59 (d, *J* = 1.79 Hz, 1H), 8.39–8.45 (m, 1H), 8.24 (d, *J* = 8.20 Hz, 1H), 8.01–8.06 (m, 2H), 7.95 (td, *J* = 1.79, 7.69 Hz, 1H), 7.67–7.73 (m, 1H), 7.61–7.67 (m, 2H), 7.53–7.57 (m, 1H), 7.50 (ddd, *J* = 1.28, 4.87, 7.69 Hz, 1H), 4.17–4.28 (m, 1H), 3.45–3.59 (m, 1H), 3.31–3.44 (m, 1H), 2.90–3.04 (m, 1H), 2.76–2.87 (m, 1H), 1.59–1.68 (m, 1H), 1.42–1.52 (m, 1H), 1.29–1.42 (m, 2H); MS (ES) *m/z* 554.0; HRMS: calculated for $C_{24}H_{22}F_3N_3O_5S_2 + H^+$, 554.10257; found (ESI, $[M+H]^+$), 554.1008; HPLC purity 94.8%, R_T 8.6 min.

5.1.3.8. 5-(Phenylsulfonyl)-*N*-[1-(pyridin-3-ylcarbonyl)piperidin-4-yl]-2-(trifluoromethyl)benzenesulfonamide (4b). ^{1}H NMR (400 MHz, DMSO-d_6) δ 8.76 (dd, *J* = 1.67, 5.00 Hz, 1H), 8.71 (dd, *J* = 0.64, 2.18 Hz, 1H), 8.67 (d, *J* = 7.17 Hz, 1H), 8.59 (d, *J* = 1.54 Hz, 1H), 8.39–8.44 (m, 1H), 8.24 (d, *J* = 8.46 Hz, 1H), 8.00–8.07 (m, 3H), 7.63–7.74 (m, 4H), 4.12–4.28 (m, 1H), 3.28–3.46 (m, 2H), 2.95–3.12 (m, 1H), 2.79–2.92 (m, 1H), 1.59–1.73 (m, 1H), 1.46–1.58 (m, 1H), 1.30–1.46 (m, 2H); MS (ES) *m/z* 554.0; HRMS: calculated for $C_{24}H_{22}F_3N_3O_5S_2 + H^+$, 554.10257; found (ESI, $[M+H]^+$), 554.1022; HPLC purity 93.8%, R_T 8.4 min.

5.1.3.9. *N*-(1-Isonicotinoylpiperidin-4-yl)-5-(phenylsulfonyl)-2-(trifluoromethyl)benzenesulfonamide (4c). ^{1}H NMR (400 MHz, DMSO-d_6) δ 8.66–8.70 (m, 2H), 8.62 (d, *J* = 7.02 Hz, 1H), 8.58 (d, *J* = 1.56 Hz, 1H), 8.41 (dd, *J* = 1.17, 8.19 Hz, 1H), 8.23 (d, *J* = 8.32 Hz, 1H), 8.01–8.06 (m, 2H), 7.67–7.73 (m, 1H), 7.62–7.67 (m, 2H), 7.31–7.38 (m, 2H), 4.19 (d, *J* = 11.44 Hz, 1H), 3.22–3.41 (m, 2H), 2.92–3.05 (m, 1H), 2.78–2.90 (m, 1H), 1.57–1.69 (m, 1H), 1.44–1.55 (m, 1H), 1.22–1.43 (m, 2H); MS (ES) *m/z* 554.1; HRMS: calculated for $C_{24}H_{22}F_3N_3O_5S_2 + H^+$, 554.10257; found (ESI, $[M+H]^+$), 554.1038; HPLC purity 99.4%, R_T 8.3 min.

5.1.3.10. *N*-{1-[(6-Chloropyridin-3-yl)carbonyl]piperidin-4-yl}-5-(phenylsulfonyl)-2-(trifluoromethyl)benzenesulfonamide (4d). ^{1}H NMR (400 MHz, DMSO-d_6) δ 8.63 (br s, 1H), 8.59 (d, *J* = 1.79 Hz, 1H), 8.44 (d, *J* = 1.79 Hz, 1H), 8.41 (d, *J* = 8.20 Hz, 1H), 8.23 (d, *J* = 8.20 Hz, 1H), 8.01–8.06 (m, 2H), 7.88 (dd, *J* = 2.31, 8.20 Hz, 1H), 7.70–7.75 (m, 1H), 7.64–7.69 (m, 2H), 7.62 (dd, *J* = 0.77, 8.20 Hz, 1H), 4.09–4.27 (m, 1H), 3.26–3.47 (m, 2H), 2.78–3.12 (m, 2H), 1.47–1.72 (m, 2H), 1.27–1.44 (m, 2H); MS (ES) *m/z* 588.0; HRMS: calculated for $C_{24}H_{21}ClF_3N_3O_5S_2 + H^+$, 588.06360; found (ESI, $[M+H]^+$), 588.0640; HPLC purity 100%, R_T 9.1 min.

5.1.3.11. 5-(Phenylsulfonyl)-2-(trifluoromethyl)-*N*-(1-{[6-(trifluoromethyl)pyridin-3-yl]carbonyl}piperidin-4-yl)benzenesulfonamide (4e). ^{1}H NMR (400 MHz, DMSO-d_6) δ 8.78 (d, *J* = 1.79 Hz, 1H), 8.65 (d, *J* = 6.66 Hz, 1H), 8.59 (d, *J* = 1.54 Hz, 1H), 8.39–8.43 (m, 1H), 8.24 (d, *J* = 8.20 Hz, 1H), 8.08–8.12 (m, 1H), 7.99–8.06 (m, 3H), 7.68–7.74 (m, 1H), 7.63–7.68 (m, 2H), 4.14–4.33 (m, 1H), 3.26–3.49 (m, 2H), 2.98–3.13 (m, 1H), 2.83–2.95 (m, 1H), 1.60–1.72 (m, 1H), 1.48–1.59 (m, 1H), 1.30–1.47 (m, 2H); MS (ES) *m/z* 621.9; HRMS: calculated for $C_{25}H_{21}F_6N_3O_5S_2 + H^+$, 622.08996; found (ESI, $[M+H]^+$), 622.0897; HPLC purity 100.0%, R_T 9.5 min.

5.1.3.12. *N*-(1-{[6-(Dimethylamino)pyridin-3-yl]carbonyl}piperidin-4-yl)-5-(phenylsulfonyl)-2-(trifluoromethyl)benzenesulfonamide (4f). ^{1}H NMR (400 MHz, DMSO-d_6) δ 8.65 (d, *J* = 7.17 Hz, 1H), 8.59 (d, *J* = 1.79 Hz, 1H), 8.42 (dd, *J* = 1.02, 8.20 Hz, 1H), 8.24 (d, *J* = 8.46 Hz, 1H), 8.01–8.11 (m, 3H), 7.71–7.79 (m, 2H), 7.63–7.71 (m, 2H), 6.97 (br s, 1H), 3.69–3.98 (m, 2H), 3.27–3.43 (m, 1H), 3.16 (s, 6H), 2.93 (m, 2H), 1.52–1.65 (m, 2H), 1.28–1.45 (m, 2H); MS (ES) *m/z* 597.0; HRMS: calculated for $C_{26}H_{27}F_3N_4O_5S_2 + H^+$, 597.14477; found (ESI, $[M+H]^+$), 597.1453; HPLC purity 100%, R_T 8.8 min.

5.1.3.13. 5-(Phenylsulfonyl)-*N*-{1-[(6-pyrrolidin-1-ylpyridin-3-yl)carbonyl]piperidin-4-yl}-2-(trifluoromethyl)benzenesulfonamide (4g). ^{1}H NMR (400 MHz, DMSO-d_6) δ 8.65 (d, *J* = 7.17 Hz, 1H), 8.59 (d, *J* = 1.54 Hz, 1H), 8.41 (d, *J* = 9.74 Hz, 1H), 8.24 (d, *J* = 8.46 Hz, 1H), 8.01–8.07 (m, 3H), 7.76 (br s, 1H), 7.73–7.79 (m, 1H), 7.64–7.71 (m, 2H), 6.89 (br s, 1H), 3.29–3.79 (m, 8H), 2.96 (br s, 1H), 1.99–2.05 (m, 4H), 1.55–1.66 (m, 2H), 1.31–1.44 (m, 2H); MS (ES) *m/z* 623.0; HRMS: calculated for $C_{28}H_{29}F_3N_4O_5S_2 + H^+$, 623.16042; found (ESI, $[M+H]^+$), 623.1609; HPLC purity 92.8%, R_T 8.9 min.

5.1.3.14. *N*-{1-[(6-Morpholin-4-ylpyridin-3-yl)carbonyl]piperidin-4-yl}-5-(phenylsulfonyl)-2-(trifluoromethyl)benzenesulfonamide (4h). ^{1}H NMR (400 MHz, DMSO-d_6) δ 8.63 (d, *J* = 7.43 Hz, 1H), 8.59 (d, *J* = 1.54 Hz, 1H), 8.39–8.44 (m, 1H), 8.24 (d, *J* = 8.46 Hz, 1H), 8.16 (d, *J* = 1.79 Hz, 1H), 8.00–8.07 (m, 2H), 7.70–7.76 (m, 1H), 7.61–7.69 (m, 3H), 6.95 (d, *J* = 8.71 Hz, 1H), 4.49 (br s, 4H), 3.65–3.75 (m, 4H), 3.52–3.61 (m, 4H), 2.83–3.00 (m, 1H), 1.50–1.61 (m, 2H), 1.25–1.41 (m, 2H); MS (ES) *m/z* 639.1; HRMS: calculated for $C_{28}H_{29}F_3N_4O_6S_2 + H^+$, 639.15534; found (ESI, $[M+H]^+$), 639.1536; HPLC purity 98.3%, R_T 9.1 min.

5.1.3.15. 5-(Phenylsulfonyl)-*N*-[1-(phenylsulfonyl)piperidin-4-yl]-2-(trifluoromethyl)benzenesulfonamide (5a). ^{1}H NMR (400 MHz, DMSO-d_6) δ 8.54 (d, *J* = 7.17 Hz, 1H), 8.50 (d, *J* = 1.54 Hz, 1H), 8.36–8.42 (m, 1H), 8.20 (d, *J* = 8.20 Hz, 1H), 7.97–8.04 (m, 2H), 7.70–7.80 (m, 4H), 7.59–7.69 (m, 4H), 3.29–3.40 (m, 2H), 2.95–3.13 (m, 1H), 2.25–2.38 (m, 2H), 1.52–1.64 (m, 2H), 1.33–1.48 (m, 2H); MS (ES) *m/z* 588.5; HRMS: calculated for $C_{24}H_{23}F_3N_2O_6S_3 + H^+$, 589.07431; found (ESI, $[M+H]^+$), 589.0731; HPLC purity 98.0%, R_T 9.8 min.

5.1.3.16. 3-{[4-({[5-(Phenylsulfonyl)-2-(trifluoromethyl)phenyl]sulfonyl}amino)piperidin-1-yl]sulfonyl}benzoic acid (5b). ^{1}H NMR (400 MHz, DMSO-d_6) δ 13.59 (br s, 1H), 8.53 (d, *J* = 7.17 Hz, 1H), 8.49 (d, *J* = 1.54 Hz, 1H), 8.36–8.41 (m, 1H), 8.23–8.28 (m, 1H), 8.20 (d, *J* = 8.46 Hz, 1H), 8.16 (t, *J* = 1.67 Hz, 1H), 7.99–8.03 (m, 2H), 7.96 (dt, *J* = 1.41, 8.20 Hz, 1H), 7.73–7.84 (m, 2H), 7.60–7.66 (m, 2H), 3.32–3.42 (m, 2H), 3.00–3.17 (m, 1H), 2.28–2.41 (m, 2H), 1.53–1.64 (m, 2H), 1.33–1.46 (m, 2H); HRMS: calculated for $C_{25}H_{23}F_3N_2O_8S_3 + H^+$, 633.06414; found (ESI, $[M+H]^+$), 633.0627; HPLC purity 100%, R_T 9.2 min.

5.1.3.17. 4-{[4-({[5-(Phenylsulfonyl)-2-(trifluoromethyl)phenyl]sulfonyl}amino)piperidin-1-yl]sulfonyl}benzoic acid (5c). ^{1}H NMR (400 MHz, DMSO-d_6) δ 13.51 (br s, 1H), 8.54 (d, *J* = 7.43 Hz, 1H), 8.49 (d, *J* = 1.79 Hz, 1H), 8.36–8.42 (m, 1H), 8.20 (d, *J* = 8.46 Hz, 1H), 8.14–8.18 (m, 2H), 7.97–8.03 (m, 2H), 7.82 (d, *J* = 8.71 Hz, 2H), 7.73–7.79 (m, 1H), 7.60–7.67 (m, 2H), 3.33–3.45 (m, 2H), 3.01–3.16 (m, 1H), 2.31–2.43 (m, 2H), 1.52–1.65 (m, 2H), 1.30–1.47 (m, 2H); MS (ES) *m/z* 632.5; HRMS: calculated for

$C_{25}H_{23}F_3N_2O_8S_3 + H^+$, 633.06414; found (ESI, $[M+H]^+$), 633.0644; HPLC purity 100%, R_T 9.2 min.

5.1.3.18. *N*-{1-[(3-Cyanophenyl)sulfonyl]piperidin-4-yl}-5-(phenylsulfonyl)-2-(trifluoromethyl)benzenesulfonamide (5d). ^{1}H NMR (400 MHz, DMSO-d_6) δ 8.54–8.61 (m, 1H), 8.50 (d, J = 2.05 Hz, 1H), 8.39 (d, J = 9.48 Hz, 1H), 8.18–8.24 (m, 3H), 7.98–8.06 (m, 3H), 7.83–7.89 (m, 1H), 7.76–7.81 (m, 1H), 7.62–7.69 (m, 2H), 3.36–3.46 (m, 2H), 3.03–3.18 (m, 1H), 2.36–2.46 (m, 2H), 1.54–1.65 (m, 2H), 1.33–1.47 (m, 2H); MS (ES) *m/z* 613.9; HPLC purity 98.4%, R_T 9.7 min.

5.1.3.19. 5-(Phenylsulfonyl)-*N*-(1-{[3-(2*H*-tetrazol-5-yl)phenyl]sulfonyl}piperidin-4-yl)-2-(trifluoromethyl)benzenesulfonamide (5e). To a stirred solution of trimethylaluminum 2 M in toluene (0.16 mL, 0.32 mmol) and trimethylsilylazide (0.04 g, 0.32 mmol) in toluene (1 mL) at 0 °C was added **5d** (0.15 g, 0.24 mmol). The resulting solution was heated to 80 °C overnight, cooled to 0 °C, quenched with 6 N HCl solution and extracted with ethyl acetate. The organic layer was concentrated and the resulting solid was flash column separated using a 0–10% MeOH/CH_2Cl_2 gradient to **5e** (0.072 g, 45%). ^{1}H NMR (400 MHz, DMSO-d_6) δ 8.55 (d, J = 7.17 Hz, 1H), 8.49 (d, J = 2.05 Hz, 1H), 8.32–8.40 (m, 3H), 8.19 (d, J = 8.46 Hz, 1H), 7.96–8.01 (m, 2H), 7.87–7.93 (m, 2H), 7.69–7.75 (m, 1H), 7.57–7.65 (m, 2H), 3.36–3.46 (m, 2H), 3.03–3.15 (m, 1H), 2.36–2.44 (m, 2H), 1.55–1.65 (m, 2H), 1.37–1.48 (m, 2H); MS (ES) *m/z* 657.0; HRMS: calculated for $C_{25}H_{23}F_3N_6O_6S_3 + H^+$, 657.08660; found (ESI, $[M+H]^+$), 657.0853; HPLC purity 93.4%, R_T 8.6 min.

5.1.3.20. 3-[4-({[5-(Phenylsulfonyl)-2-(trifluoromethyl)phenyl]sulfonyl}amino)piperidin-1-yl]benzoic acid (6a). ^{1}H NMR (400 MHz, DMSO-d_6) δ 8.56–8.64 (m, 2H), 8.40–8.46 (m, 1H), 8.25 (d, J = 8.46 Hz, 1H), 8.01–8.09 (m, 2H), 7.74–7.81 (m, 1H), 7.66–7.73 (m, 2H), 7.50 (br s, 1H), 7.32–7.44 (m, 2H), 7.19–7.28 (m, 1H), 3.49–3.64 (m, 2H), 3.19–3.34 (m, 1H), 2.68–2.86 (m, 2H), 1.43–1.69 (m, 4H); HRMS: calculated for $C_{25}H_{23}F_3N_2O_6S_2 + H^+$, 569.10224; found (ESI, $[M+H]^+$), 569.1022; HPLC purity 100%, R_T 9.7 min.

5.1.3.21. 4-[4-({[5-(Phenylsulfonyl)-2-(trifluoromethyl)phenyl]sulfonyl}amino)piperidin-1-yl]benzoic acid (6b). ^{1}H NMR (400 MHz, DMSO-d_6) δ 8.50–8.64 (m, 2H), 8.37–8.46 (m, 1H), 8.25 (d, J = 8.20 Hz, 1H), 8.01–8.08 (m, 2H), 7.73–7.82 (m, 3H), 7.64–7.72 (m, 2H), 6.92 (d, J = 9.22 Hz, 2H), 3.64–3.80 (m, 2H), 3.20–3.38 (m, 1H), 2.72–2.86 (m, 2H), 1.52–1.64 (m, 2H), 1.35–1.48 (m, 2H); HRMS: calculated for $C_{25}H_{23}F_3N_2O_6S_2 + H^+$, 569.10224; found (ESI, $[M+H]^+$), 569.0995.

5.1.3.22. 2-[4-({[5-(Phenylsulfonyl)-2-(trifluoromethyl)phenyl]sulfonyl}amino)piperidin-1-yl]acetamide (7a). ^{1}H NMR (400 MHz, DMSO-d_6) δ 8.51–8.61 (m, 2H), 8.41 (dd, J = 1.03, 8.20 Hz, 1H), 8.23 (d, J = 8.46 Hz, 1H), 7.99–8.07 (m, 2H), 7.74–7.82 (m, 1H), 7.64–7.72 (m, 2H), 7.10 (br s, 2H), 2.89–3.02 (m, 1H), 2.77 (s, 2H), 2.62 (d, J = 12.04 Hz, 2H), 1.83–1.98 (m, 2H), 1.37–1.50 (m, 4H); HRMS: calculated for $C_{20}H_{22}F_3N_3O_5S_2 + H^+$, 506.10257; found (ESI, $[M+H]^+$), 506.103; HPLC purity 98.6%, R_T 6.8 min.

5.1.3.23. [4-({[5-(Phenylsulfonyl)-2-(trifluoromethyl)phenyl]sulfonyl}amino)piperidin-1-yl]acetic acid (7b). A stirred solution of **1** (0.14 g, 0.30 mmol) and *tert*-butylbromoacetate (0.06 g, 0.30 mmol) and triethylamine (0.1 mL, 0.7 mmol) in THF (1 mL) was microwave irradiated for 10 min at 120 °C. The resulting solution was concentrated and flash column separation using 0–50% ethyl acetate/hexane gradient gave a solid. The solid was dissolved in 4 N HCl in dioxane solution (1 mL) and stirred overnight. The solution was concentrated and trituration with ethyl acetate gave **7b** (0.09 g, 59%). ^{1}H NMR (400 MHz, DMSO-d_6) δ 8.84 (d, J = 6.92 Hz, 1H), 8.59 (d, J = 1.54 Hz, 1H), 8.41 (dd, J = 1.28, 8.20 Hz, 1H), 8.24 (d, J = 8.46 Hz, 1H), 8.00–8.10 (m, 2H), 7.75–7.84 (m, 1H), 7.65–7.74 (m, 2H), 4.00 (br s, 2H), 3.34 (br s, 4H), 3.02 (br s, 1H), 1.81 (br s, 4H); HRMS: calculated for $C_{20}H_{21}F_3N_2O_6S_2 + H^+$, 507.08659; found (ESI, $[M+H]^+$), 507.0854; HPLC purity 100%, R_T 6.8 min.

5.1.3.24. 3-[4-({[5-(Phenylsulfonyl)-2-(trifluoromethyl)phenyl]sulfonyl}amino)piperidin-1-yl]propanoic acid (7c). ^{1}H NMR (400 MHz, DMSO-d_6) δ 8.78–8.90 (m, 1H), 8.58 (d, J = 1.79 Hz, 1H), 8.42 (dd, J = 1.15, 8.07 Hz, 1H), 8.25 (d, J = 8.20 Hz, 1H), 8.02–8.08 (m, 2H), 7.77–7.83 (m, 1H), 7.68–7.75 (m, 2H), 3.24–3.46 (m, 4H), 3.18 (br s, 2H), 2.89 (br s, 1H), 2.76 (t, J = 7.43 Hz, 2H), 1.77 (br s, 4H); HRMS: calculated for $C_{21}H_{23}F_3N_2O_6S_2 + H^+$, 521.10224; found (ESI, $[M+H]^+$), 521.1035; HPLC purity 97.6%, R_T 6.8 min.

5.1.3.25. 4-Oxo-4-[4-({[5-(phenylsulfonyl)-2-(trifluoromethyl)-phenyl]sulfonyl}amino)piperidin-1-yl]butanoic acid (7d). A stirred solution of 5-(phenylsulfonyl)-*N*-piperidin-4-yl-2-(trifluoromethyl)benzenesulfonamide (0.10 g, 0.22 mmol) and succinic anhydride (0.023 g, 0.23 mmol) in EtOH (1 mL) was microwave irradiated for 10 min at 150 °C. The resulting solution was concentrated and flash column separation using 0–10% methanol/methylene chloride gradient afforded **7d** (0.04 g, 33%). ^{1}H NMR (400 MHz, DMSO-d_6) δ 8.45–8.70 (br s, 1H), 8.58 (d, J = 1.79 Hz, 1H), 8.42 (d, J = 9.48 Hz, 1H), 8.24 (d, J = 8.20 Hz, 1H), 8.01–8.07 (m, 2H), 7.75–7.82 (m, 1H), 7.66–7.73 (m, 2H), 4.01–4.13 (m, 1H), 3.62–3.74 (m, 1H), 2.87–2.99 (m, 1H), 2.35–2.43 (m, 2H), 1.52–1.61 (m, 1H), 1.42–1.51 (m, 1H), 1.23–1.38 (m, 1H), 1.09–1.21 (m, 1H); MS (ESI) *m/z* 549; HRMS: calculated for $C_{22}H_{23}F_3N_2O_7S_2 + H^+$, 549.09715; found (ESI, $[M+H]^+$), 549.095; HPLC purity 100%, R_T 8.1 min.

5.1.3.26. 5-Oxo-5-[4-({[5-(phenylsulfonyl)-2-(trifluoromethyl)-phenyl]sulfonyl}amino)piperidin-1-yl]pentanoic acid (7e). ^{1}H NMR (400 MHz, DMSO-d_6) δ 12.01 (br s, 1H), 8.54–8.61 (m, 2H), 8.42 (dd, J = 1.02, 8.20 Hz, 1H), 8.24 (d, J = 8.20 Hz, 1H), 8.01–8.07 (m, 2H), 7.75–7.82 (m, 1H), 7.66–7.73 (m, 2H), 4.04–4.15 (m, 1H), 3.60–3.71 (m, 1H), 3.21–3.29 (m, 1H), 2.85–2.98 (m, 1H), 2.16–2.35 (m, 4H), 1.63–1.75 (m, 2H), 1.43–1.59 (m, 2H), 1.11–1.34 (m, 2H); HRMS: calculated for $C_{23}H_{25}F_3N_2O_7S_2 + H^+$, 563.11280; found (ESI, $[M+H]^+$), 563.1128; HPLC purity 100%, R_T 8.2 min.

5.1.3.27. *N*-[1-(2-Hydroxyethyl)piperidin-4-yl]-5-(phenylsulfonyl)-2-(trifluoromethyl)benzenesulfonamide (7f). To a stirred solution of **1** (0.09 g, 0.20 mmol) in 1,4-dioxane (1 mL) was added 2-bromoethanol (0.05, 0.40 mmol) and triethylamine (0.1 mL, 0.7 mmol). The resulting solution was heated 150 °C in a microwave for 10 min and concentrated. Flash column separation using 0–5% methanol/methylene chloride gradient gave **7f** (0.03 g, 30%). ^{1}H NMR (400 MHz, DMSO-d_6) δ 8.57 (d, J = 1.54 Hz, 1H), 8.39–8.44 (m, 1H), 8.24 (d, J = 8.46 Hz, 1H), 8.01–8.06 (m, 2H), 7.76–7.82 (m, 1H), 7.67–7.73 (m, 2H), 3.53 (br s, 4H), 2.81–3.17 (m, 6H), 1.30–1.97 (m, 4H); MS (ES) *m/z* 493.1; HRMS: calculated for $C_{20}H_{23}F_3N_2O_5S_2 + H^+$, 493.10732; found (ESI, $[M+H]^+$), 493.1083; HPLC purity 98.3%, R_T 6.8 min.

5.1.3.28. *N*-[1-(2-Hydroxy-2-methylpropyl)piperidin-4-yl]-5-(phenylsulfonyl)-2-(trifluoromethyl)benzenesulfonamide (7g).

To a stirred mixture of **1** (0.075 g, 0.167 mmol) in ethanol (2 mL) was added isobutylene oxide (0.05 g, 0.69 mmol) and the resulting mixture was heated to reflux overnight. The crude

mixture was concentrated and purified using flash column chromatography employing 50–100% ethyl acetate/hexane gradient and afforded **7g** (0.06 g, 70%). ^{1}H NMR (400 MHz, DMSO-d_6) δ 8.57 (d, J = 1.82 Hz, 1H), 8.48 (d, J = 7.28 Hz, 1H), 8.41 (dd, J = 1.17, 8.19 Hz, 1H), 8.23 (d, J = 8.32 Hz, 1H), 8.01–8.06 (m, 2H), 7.74–7.80 (m, 1H), 7.66–7.72 (m, 2H), 4.02 (s, 1H), 2.85–2.98 (m, 1H), 2.69–2.78 (m, 2H), 2.09 (s, 2H), 1.88–1.98 (m, 2H), 1.35–1.45 (m, 4H), 1.05 (s, 6H); MS (ES) *m/z* 519.0; HRMS: calculated for $C_{22}H_{27}F_3N_2O_5S_2 + H^+$, 521.13862; found (ESI, $[M+H]^+$), 521.1403; HPLC purity 96.8%, R_T 7.1 min.

5.1.3.29. *tert*-Butyl 4-{[4-({[5-(phenylsulfonyl)-2-(trifluoromethyl)phenyl]sulfonyl}amino)piperidin-1-yl]carbonyl}piperidine-1-carboxylate (8a). ^{1}H NMR (400 MHz, DMSO-d_6) δ 8.59 (d, J = 1.54 Hz, 1H), 8.57 (d, J = 7.18 Hz, 1H), 8.42 (dd, J = 1.28, 8.20 Hz, 1H), 8.24 (d, J = 8.46 Hz, 1H), 8.02–8.08 (m, 2H), 7.75–7.81 (m, 1H), 7.66–7.73 (m, 2H), 4.05–4.16 (m, 1H), 3.86–3.99 (m, 2H), 3.75–3.85 (m, 1H), 2.91–3.05 (m, 1H), 2.69–2.87 (m, 4H), 2.52–2.62 (m, 1H), 1.45–1.68 (m, 4H), 1.39 (s, 9H), 1.26–1.37 (m, 3H), 1.10–1.22 (m, 1H); MS (ES) *m/z* 657.8; HRMS: calculated for $C_{29}H_{36}F_3N_3O_7S_2 + H^+$, 660.20195; found (ESI, $[M+H]^+$), 660.2032; HPLC purity 100%, R_T 9.8 min.

5.1.3.30. *tert*-Butyl 4-{2-oxo-2-[4-({[5-(phenylsulfonyl)-2-(trifluoromethyl)phenyl]sulfonyl}amino)piperidin-1-yl]ethyl}piperidine-1-carboxylate (8b). ^{1}H NMR (400 MHz, DMSO-d_6) δ 8.58 (d, J = 1.79 Hz, 1H), 8.56 (br s, 1H), 8.41 (dd, J = 1.02, 7.94 Hz, 1H), 8.24 (d, J = 8.46 Hz, 1H), 8.02–8.07 (m, 2H), 7.75–7.81 (m, 1H), 7.66–7.73 (m, 2H), 4.07–4.16 (m, 1H), 3.84–3.95 (m, 2H), 3.67–3.77 (m, 1H), 3.24–3.30 (m, 1H), 2.88–3.00 (m, 1H), 2.61–2.81 (m, 2H), 2.21 (d, J = 6.15 Hz, 2H), 1.77–1.89 (m, 1H), 1.54–1.67 (m, 4H), 1.44–1.52 (m, 1H), 1.38 (s, 9H), 1.25–1.34 (m, 1H), 1.13–1.21 (m, 1H), 0.95–1.06 (m, 2H); HRMS: calculated for $C_{30}H_{38}F_3N_3O_7S_2 + H^+$, 674.21760; found (ESI, $[M+H]^+$), 674.2167; HPLC purity 97.7%, R_T 10.0 min.

5.1.3.31. *tert*-Butyl (3*S*)-3-{[4-({[5-(phenylsulfonyl)-2-(trifluoromethyl)phenyl]sulfonyl}amino)piperidin-1-yl]carbonyl}pyrrolidine-1-carboxylate (8e). ^{1}H NMR (400 MHz, DMSO-d_6) δ 8.53–8.61 (m, 2H), 8.42 (dd, J = 1.15, 8.33 Hz, 1H), 8.24 (d, J = 8.46 Hz, 1H), 8.01–8.09 (m, 2H), 7.75–7.82 (m, 1H), 7.65–7.73 (m, 2H), 4.05–4.16 (m, 1H), 3.74–3.86 (m, 1H), 3.17–3.47 (m, 5H), 2.92–3.06 (m, 1H), 2.54–2.64 (m, 1H), 1.76–2.03 (m, 3H), 1.57–1.66 (m, 1H), 1.45–1.56 (m, 1H), 1.36–1.43 (m, 9H), 1.28–1.35 (m, 1H), 1.15–1.23 (m, 1H); HRMS: calculated for $C_{28}H_{34}F_3N_3O_7S_2 + H^+$, 646.18630; found (ESI, $[M+H]^+$), 646.1891; HPLC purity 100.0%, R_T 9.8 min.

5.1.3.32. *tert*-Butyl (3*R*)-3-{[4-({[5-(phenylsulfonyl)-2-(trifluoromethyl)phenyl]sulfonyl}amino)piperidin-1-yl]carbonyl}pyrrolidine-1-carboxylate (8f). ^{1}H NMR (400 MHz, DMSO-d_6) δ 8.53–8.61 (m, 2H), 8.42 (d, J = 8.71 Hz, 1H), 8.24 (d, J = 8.46 Hz, 1H), 8.01–8.08 (m, 2H), 7.75–7.82 (m, 1H), 7.63–7.74 (m, 2H), 4.06–4.15 (m, 1H), 3.73–3.87 (m, 1H), 3.17–3.47 (m, 5H), 2.92–3.04 (m, 1H), 2.54–2.63 (m, 1H), 1.74–2.01 (m, 3H), 1.57–1.67 (m, 1H), 1.47–1.56 (m, 1H), 1.37–1.42 (m, 9H), 1.26–1.36 (m, 1H), 1.11–1.24 (m, 1H); HRMS: calculated for $C_{28}H_{34}F_3N_3O_7S_2 + H^+$, 646.18630; found (ESI, $[M+H]^+$), 646.189; HPLC purity 100.0%, R_T 9.8 min.

5.1.4. General procedure for the acid catalyzed hydrolysis of tertiary butyl esters

5.1.4.1. 5-(Phenylsulfonyl)-*N*-[1-(piperidin-4-ylcarbonyl)piperidin-4-yl]-2-(trifluoromethyl)benzenesulfonamide (8g). To a stirred solution of **8a** (0.10 g, 0.15 mmol) in ethyl acetate (2 mL) was bubbled HCl gas. The resulting solution was stirred at room temperature overnight, and concentrated. The resulting solid was triturated with diethyl ether and provided **8g** as a white solid (0.085 g, 85%). ^{1}H NMR (400 MHz, DMSO-d_6) δ 8.83 (br s, 1H), 8.63 (d, J = 7.17 Hz, 1H), 8.60 (d, J = 1.79 Hz, 1H), 8.46–8.57 (m, 1H), 8.40–8.44 (m, 1H), 8.24 (d, J = 8.20 Hz, 1H), 8.03–8.07 (m, 2H), 7.76–7.81 (m, 1H), 7.67–7.73 (m, 2H), 4.04–4.16 (m, 1H), 3.77–3.88 (m, 1H), 3.20–3.36 (m, 4H), 2.97–3.06 (m, 1H), 2.85–2.97 (m, 3H), 2.54–2.63 (m, 1H), 1.63–1.80 (m, 5H), 1.49–1.56 (m, 1H), 1.29–1.40 (m, 1H), 1.14–1.26 (m, 1H); MS (ES) *m/z* 559.8; HRMS: calculated for $C_{24}H_{28}F_3N_3O_5S_2 + H^+$, 560.14952; found (ESI, $[M+H]^+$), 560.1478; HPLC purity 100%, R_T 7.2 min.

5.1.4.2. 5-(Phenylsulfonyl)-*N*-[1-(piperidin-4-ylacetyl)piperidin-4-yl]-2-(trifluoromethyl)benzenesulfonamide (8h). ^{1}H NMR (400 MHz, DMSO-d_6) δ 8.55–8.65 (m, 3H), 8.30–8.46 (m, 2H), 8.24 (d, J = 8.20 Hz, 1H), 8.02–8.07 (m, 2H), 7.75–7.82 (m, 1H), 7.66–7.73 (m, 2H), 3.66–4.19 (m, 1H), 3.17–3.35 (m, 4H), 2.77–3.01 (m, 4H), 2.54–2.63 (m, 1H), 2.26 (d, J = 6.66 Hz, 2H), 1.88–2.02 (m, 1H), 1.74–1.84 (m, 2H), 1.45–1.68 (m, 1H), 1.10–1.40 (m, 4H); MS (ES) *m/z* 573.9; HRMS: calculated for $C_{25}H_{30}F_3N_3O_5S_2 + H^+$, 574.16517; found (ESI, $[M+H]^+$), 574.1636; HPLC purity 98.0%, R_T 7.3 min.

5.1.4.3. 5-(Phenylsulfonyl)-*N*-{1-[(3*S*)-pyrrolidin-3-ylcarbonyl]-piperidin-4-yl}-2-(trifluoromethyl)benzenesulfonamide (8k). ^{1}H NMR (400 MHz, DMSO-d_6) δ 9.19 (br s, 1H), 9.00 (br s, 1H), 8.65 (dd, J = 7.30, 17.30 Hz, 1H), 8.60 (d, J = 1.54 Hz, 1H), 8.42 (d, J = 7.94 Hz, 1H), 8.25 (d, J = 8.20 Hz, 1H), 8.02–8.09 (m, 2H), 7.76–7.83 (m, 1H), 7.67–7.74 (m, 2H), 4.05–4.19 (m, 1H), 3.73–3.82 (m, 1H), 3.42–3.53 (m, 1H), 3.10–3.39 (m, 4H), 2.96–3.08 (m, 1H), 2.60–2.71 (m, 1H), 2.11–2.25 (m, 1H), 1.76–1.90 (m, 1H), 1.60–1.73 (m, 2H), 1.50–1.60 (m, 1H), 1.31–1.42 (m, 1H), 1.18–1.29 (m, 1H); HPLC purity 90.4%, R_T 7.3 min.; HRMS: calculated for $C_{23}H_{26}F_3N_3O_5S_2 + H^+$, 546.13387; found (ESI, $[M+H]^+$), 546.1302.

5.1.4.4. 5-(Phenylsulfonyl)-*N*-{1-[(3*R*)-pyrrolidin-3-ylcarbonyl]-piperidin-4-yl}-2-(trifluoromethyl)benzenesulfonamide (8l). ^{1}H NMR (400 MHz, DMSO-d_6) δ 9.00 (br s, 2H), 8.56–8.70 (m, 2H), 8.42 (d, J = 8.71 Hz, 1H), 8.25 (d, J = 8.20 Hz, 1H), 8.01–8.08 (m, 2H), 7.75–7.84 (m, 1H), 7.65–7.74 (m, 2H), 4.03–4.16 (m, 1H), 3.72–3.82 (m, 1H), 3.43–3.53 (m, 1H), 3.10–3.41 (m, 4H), 2.96–3.08 (m, 1H), 2.62–2.72 (m, 1H), 2.10–2.24 (m, 1H), 1.75–1.90 (m, 1H), 1.61–1.73 (m, 2H), 1.52–1.60 (m, 1H), 1.30–1.44 (m, 1H), 1.17–1.29 (m, 1H); HRMS: calculated for $C_{23}H_{26}F_3N_3O_5S_2$ H^+, 546.13387; found (ESI, $[M+H]^+$), 546.1336; HPLC purity 95.7%, R_T 7.3 min.

6. sFRP-1 In vitro characterization assays

6.1. Fluorescence polarization binding assay

The affinity of test compounds for sFRP-1 was determined using a fluorescence polarization binding assay. According to the assay design, a probe compound was bound to sFRP-1. The fluorescence anisotropy value of the probe compound increased upon binding to sFRP-1. Upon the addition of a test compound, the fluorescence anisotropy value for the probe compound decreased due to competitive displacement of the probe by the test compound. The decrease in anisotropy as a function of increasing concentration of the test compound provided a direct measure of the test compound's binding affinity for sFRP-1.

To determine IC_{50} values, fluorescence polarization experiments were conducted in a 384-well format according to the following procedures. A 20 mM stock solution of the probe

compound was prepared in 100% DMSO and dispensed in 10 μL aliquots for long-term storage at −20 °C. The binding assay buffer was prepared by combining stock solutions of Tris–Cl, NaCl, glycerol, and NP40 at final concentrations of 25 mM Tris–Cl pH 7.4, 0.5 M NaCl, 5% glycerol and 0.002% NP40. Master stock solutions of the test compounds were prepared in 100% DMSO at final concentrations of 20 mM. Typically the working stock solutions of the test compounds were prepared by serially diluting the 20 mM master stock solution to 5 mM, 2.5 mM, 1.25 mM, 0.625 mM, 0.3125 mM, 0.156 mM, 78 μM, 39 μM, 19.5 μM, 9.8 μM, 4.9 μM, 2.44 μM, 1.22 μM, 0.31 μM, 76 nM, and 19 nM in DMSO. The working stock solutions of the test compounds were further diluted by combining 6 μL of the solutions with 24 μL of Milli-Q purity water, resulting in working stock solutions (10× compound stocks) in 20% DMSO.

The assay controls were prepared as follows. A 2 μL aliquot of the 20 mM fluorescence probe compound was diluted 1000-fold in 100% DMSO to a final concentration of 20 μM. Six microliters of the 20 μM probe were combined with 5.4 mL of the assay buffer, mixed well, and 18 μL of the resulting solution was dispensed into 384-well plates.

sFRP-1/probe complex was prepared by combining 11 μL of 20 μM probe compound with 9.9 mL of the assay buffer and sFRP-1 stock solution to final concentrations of 22 nM probe compound and 50 nM sFRP-1. Eighteen microliters of the sFRP-1/probe complex were dispensed into the 384-well plates.

Aliquots of the test compounds from the 10x working stock solutions (2 μL) were removed and dispensed into the plate containing the sFRP-1/probe complex and the resultant solutions were mixed by pipetting 10 μL up and down twice. The final concentrations of sFRP-1 and probe in the assay solutions were 45 nM and 20 nM, respectively. In a typical experiment, each plate was used to test 14 compounds.

The plate was incubated in the dark for 30 min. The fluorescence of the sFRP-1/probe complexes was read in the Tecan Ultra plate reader at excitation and emission maxima of 485 and 535 nm.

Fluorescence anisotropy results from the emission of polarized light in the parallel and perpendicular directions when a fluorophore is excited with vertically polarized light. The anisotropy of the probe in the free and bound state was determined using the following equation: $r = [I(\mathrm{II}) - I(\perp)] \div [I(\mathrm{II}) + 2I(\perp)]$, where $I(\mathrm{II})$ and $I(\perp)$ are the parallel and perpendicular emission intensities, respectively.

Monitoring the anisotropy changes of the probe compound revealed that it bound saturably to sFRP-1 with a K_D of 20–30 nM. The binding affinity was independently verified using a tryptophan fluorescence-quenching assay.

The decrease in the anisotropy of the probe upon addition of the competing test compound was fitted to a sigmoidal dose–response curve of the equation shown below: $Y = \mathrm{Bottom} + \frac{(\mathrm{Top}-\mathrm{Bottom})}{(1+10^{X-\mathrm{Log\ IC_{50}}})} * \mathrm{Hillslope}$, where '*X*' is the logarithm of concentration, '*Y*' is the anisotropy, and 'Bottom' and 'Top' correspond to the anisotropy values of the free and sFRP-1-bound probe prior to the addition of the test compound, respectively.

For automated IC_{50} determinations, the equation shown above was used in the program GraphPad Prism. The 'Hillslope' was kept constant at 1. The value for 'Bottom' was fixed, but was determined by the blank (probe-only) wells in the plate. The values for 'Top' and 'IC_{50}' were determined by the data fit. The value for 'Top' was typically close to 120, equivalent to approximately 50% bound probe, and the value for 'Bottom' was around 30, due to free probe. If the test compound interfered with the probe in the fluorescence assay at high concentrations, the range for the fitted data was limited to the lower concentration range.

6.2. Cell-based, TCF-reporter functional assay

U2-OS bone cells are infected with recombinant adenovirus 5 (Ad5)-WNT3 at a multiplicity of infection (MOI) of 2, followed by infection with Ad5-sFRP-1 and Ad5-16xTCF-luciferase, each at an MOI of 10. Four hours after infection, the cells are frozen in sterile cryogenic vials at a cell density of 9E+6 cells/mL and stored in a −150 °C freezer. For the assay, a vial of frozen cells is thawed, and the cells are resuspended in plating medium [phenol red-free RPMI 1640 medium containing 5% fetal calf serum, 2 mM GlutaMAX-l, and 1% (v/v) penicillin–streptomycin] to a final cell density of 1.5E+5 cells/mL. The resuspended cells are then plated in 96-well tissue culture treated plates at a volume of 100 μL of cell suspension/well (i.e., 1.5E+4 cells/well). The plates are incubated at 37 °C inside a 5% CO_2/95% humidified air incubator for 5 h or until the cells have attached and started to spread. Prior to the addition of test compounds, the medium is replaced with 50 μL/well of phenol red-free RPMI 1640 containing 10% fetal calf serum, 2 mM GlutaMAX-l, and 1% (v/v) penicillin–streptomycin. Test compounds, or vehicle (typically DMSO), diluted in phenol red-free RPMI 1640 containing 2 mM GlutaMAX-l, and l% (v/v) penicillin–streptomycin are then added to the wells in replicates of 4 wells/dilution and the plates are incubated at 37 °C overnight. Dose–response experiments are performed with the compounds in twofold serial dilutions from 10,000 to 4.9 nM. After the overnight incubation, the cells are washed twice with 150 μL/well of PBS w/o calcium or magnesium and lysed with 50 μL/well of 1× cell culture lysis reagent (Promega Corporation) on a shaker at room temperature for 30 min. Aliquots of the cell lysates (30 μL) are transferred to 96-well luminometer plates, and the luciferase activity is measured in a MicroLumat PLUS luminometer (EG&G Berthold) using 100 μL/well of luciferase substrate (Promega Corporation).

Following the injection of substrate, luciferase activity is measured for 10 s after a 1.6 s delay. The luciferase activity data is transferred from the luminometer to a PC and analyzed using the SAS/EXCEL program to determine EC_{50} values. The luciferase data is analyzed using the SAS/EXCEL program. EC_{50} determinations for dose–response curves are determined using the SAS/EXCEL program.

7. Ex vivo bone formation assay

Neonatal mouse calvaria were prepared from 4-day-old pups as described previously.[14] Briefly, calvaria were excised and cut in half along the sagittal suture. Calvaria were incubated overnight in serum-free BGJ medium containing 0.1% (w/v) bovine serum albumin (BSA). Each half calvaria was placed with the concave surface downward on a stainless steel grid (Small Parts Inc, Miami, FL) in a 12-well tissue culture dish (Becton Dickinson, Oxnard, CA). Each well contained 1.0 mL of BGJ medium with 1.0% (v/v) fetal bovine serum (FBS). Calvaria were incubated for seven days with 0.1% (v/v) dimethyl sulfoxide (DMSO, vehicle control) or with compounds in a humidified atmosphere of 95% air and 5% CO_2, and the medium was changed on day 4 with fresh DMSO or compounds added.

After organ culture, calvaria were fixed in 10% neutral phosphate-buffered formaldehyde at room temperature for at least 72 h, then decalcified for 6 h in 10% EDTA in phosphate-buffered saline (PBS). Calvaria were embedded in parallel in the same paraffin block, and 4 μm sections were stained with hematoxylin-eosin. Consistent bone areas (200 μm away from the frontal sutures) were selected for histomorphometric analysis. A 200 μm square grid was placed on each calvarium, and total bone area, as well as the number of osteoblasts within the grid, was determined with the Osteomeasure System (Osteometrics Inc, Atlanta, GA). All cells on the bone surface were counted as osteoblasts. Data were

analyzed for statistical significance by one-way ANOVA using the Dunnett's test with JMP software (SAS Institute, Cary, NC).

Acknowledgments

The authors wish to thank the Departments of Analytical Chemistry and Chemical Technologies, Wyeth, for analytical and profile data. We also wish to thank our management, Drs. M. Abou-Gharbia, T. Mansour and L. Freedman, for their support of this work.

References and notes

1. Wodarz, A.; Nusse, R. *Ann. Rev. Cell Dev. Biol.* **1998**, *14*, 59.
2. Baron, R.; Rawadi, G.; Roman-Roman, S. *Curr. Top. Dev. Biol.* **2006**, *76*, 103.
3. (a) Li, C. H.; Amar, S. *J. Dent. Res.* **2006**, *85*, 374; (b) Kumar, S.; Leontovich, A.; Coenen, M. J.; Bahn, R. S. *J. Clin. Endocrinol. Metab.* **2005**, *90*, 4730; (c) Wang, W.-H.; McNatt, L. G.; Pang, I.-H.; Millar, J. C.; Hellberg, P. E.; Hellberg, M. H.; Steely, H. T.; Rubin, J. S.; Fingert, J. H.; Sheffield, V. C.; Stone, E. M.; Clark, A. F. *J. Clin. Invest.* **2008**, *118*, 1056.
4. (a) Kulkarni, N. H.; Halladay, D. L.; Miles, R. R.; Gilbert, L. M.; Frolik, C. A.; Galvin, R. J. S.; Martin, T. J.; Gillespie, M. T.; Onyia, J. E. *J. Cell. Biochem.* **2005**, *95*, 1178; (b) Bodine, P. V. N.; Seestaller-Wehr, L.; Kharode, Y. P.; Bex, F. J.; Komm, B. S. *J. Cell. Phys.* **2007**, *210*, 352.
5. Kawano, Y.; Kypta, R. *J. Cell Sci.* **2003**, *116*, 2627.
6. (a) Rattner, A.; Hsieh, J. C.; Smallwood, P. M.; Gilbert, D. J.; Copeland, N. G.; Jenkins, N. A.; Nathans, J. *Proc. Natl. Acad. Sci.* **1997**, *94*, 2859; (b) Jones, S. E.; Jomary, C. *BioEssays* **2002**, *24*, 811; (c) Chong, J. M.; Uren, A.; Rubin, J. S.; Speicher, D. W. *J. Biol. Chem.* **2002**, *277*, 5134.
7. (a) Roman-Roman, S.; Shi, D.-L.; Stiot, V.; Hay, E.; Vayssiere, B.; Garcia, T.; Baron, R.; Rawadi, G. M. *J. Biol. Chem.* **2004**, *279*, 5725; (b) Bodine, P. V. N. *J. Musculoskelet. Neuronal Interact.* **2008**, *8*, 296; (c) Gaur, T.; Wixted, J. J.; Hussain, S.; O'Connell, S. L.; Morgan, E. F.; Ayers, D. C.; Komm, B. S.; Bodine, P. V.; Stein, G. S.; Lian, J. B. *J. Cell Phys.* **2009**, *220*, 174.
8. Gopalsamy, A.; Shi, M.; Stauffer, B.; Bahat, R.; Billiard, J.; Ponce-de-Leon, H.; Seestaller-Wehr, L.; Fukayama, S.; Mangine, A.; Moran, R.; Krishnamurthy, G.; Bodine, P. *J. Med. Chem.* **2008**, *51*, 7670.
9. Moore, W. J.; Kern, J. C.; Bhat, R.; Commons, T. J.; Fukayama, S.; Goljer, I.; Krishnamurthy, G.; Magolda, R. L.; Nogle, L.; Pitts, K.; Stauffer, B.; Trybulski, E. J.; Welmaker, G. S.; Wilson, M.; Bodine, P. V. N. *J. Med. Chem.* **2009**, *52*, 105.
10. Zhong, X.; Desilva, T.; Lin, L.; Bodine, P.; Bhat, R. A.; Presman, E.; Pocas, J.; Stahl, M.; Kriz, R. *J. Biol. Chem.* **2007**, *282*, 20523.
11. (a) Moore, W. J.; Kern, J. C.; Commons, T. J.; Wilson, M. A.; Welmaker, G. S.; Trybulski, E. J.; Pitts, K.; Krishnamurthy, G.; Stauffer, B.; Bhat, R.; Fukayama, S.; Upthagrove, A. L.; Bodine, P. V. N. *Abstracts of Papers*, 234th National Meeting of the American Chemical Society, Boston, MA, August 19–23, 2007; American Chemical Society: Washington, DC; MEDI-385.; (b) Kern, J. C.; Moore, W. J.; Commons, T. J.; Woodworth, R. P.; Wilson, M. A.; Welmaker, G. S.; Trybulski, E. J.; Pitts, K.; Krishnamurthy, G.; Stauffer, B.; Bhat, R.; Bodine, P. V. N. *Abstracts of Papers*, 234th National Meeting of the American Chemical Society, Boston, MA, August 19–23, 2007; American Chemical Society: Washington, DC; MEDI-387.; (c) Welmaker, G. S.; Wilson, M. A.; Moore, W. J.; Kern, J. C.; Trybulski, E. J.; Magolda, R. L.; Pitts, K.; Krishnamurthy, G.; Stauffer, B.; Bhat, R.; Bodine, P. V. N. *Abstracts of Papers*, 234th National Meeting of the American Chemical Society, Boston, MA, August 19–23, 2007; American Chemical Society: Washington, DC; MEDI-389.
12. Gopalsamy, A.; Moore, W. J.; Kern, J. C.; Molinari, A. J.; Shi, M.; Welmaker, G. S.; Wilson, M. A.; Krishnamurthy, G.; Commons, T. J.; Webb, M. B.; Woodworth, R. P. U.S. PCT 2006/0276464.
13. Huff, B. E.; Staszak, M. A. *Tetrahedron Lett.* **1993**, *34*, 8011.
14. (a) Mundy, G.; Garrett, R.; Harris, S.; Chan, J.; Chen, D.; Rossini, G.; Boyce, B.; Zhao, M.; Gutierrez, G. *Science* **1999**, *286*, 1946; (b) Traianedes, K.; Dallas, M. R.; Garrett, I. R.; Mundy, G. R.; Bonewald, L. F. *Endocrinology* **1998**, *139*, 3178.
15. Despite the good solubility and in vitro microsomal stability, compound **5b** demonstrated efflux properties in a Caco-2 model for intestinal absorption. This observation is consistent with a model of bioavailability that was established for negatively charged compounds at pH 6: Martin, Y. C. A. *J. Med. Chem.* **2005**, *48*, 3164.